

High overtones of Dirac perturbations of a Schwarzschild black hole

K. H. C. Castello-Branco

Universidade de São Paulo, Instituto de Física
Caixa Postal 66318, 05315-970, São Paulo-SP, Brazil.
karlucio@fma.if.usp.br

R.A. Konoplya

Universidade de São Paulo, Instituto de Física
Caixa Postal 66318, 05315-970, São Paulo-SP, Brazil.
konoplya@fma.if.usp.br

and

A. Zhidenko

Department of Physics, Dniepropetrovsk National University
St. Naukova 13, Dniepropetrovsk 49050, Ukraine.
Z_A_V@ukr.net

Abstract

Using the Fröbenius method, we find high overtones of Dirac perturbations of the Schwarzschild black hole quasinormal spectrum. It is shown that at high overtones the quasinormal behavior is quite different from that for fields of integer spin. In particular, for Dirac perturbations the spacing for imaginary part of ω_n approach an equidistant regime $Im\omega_{n+1} - Im\omega_n = i/8M$, where M is the mass of the black hole. At higher overtones the real part of ω goes to zero. In addition, at lower overtones, we have found “specific modes” which have the imaginary part equal to $i/8M$ for any multipole number. These modes are apparently “algebraically special” modes. The values for lower overtones found by Fröbenius technique are in excellent agreement with those obtained through the WKB formula.

1 Introduction

The Quasinormal Mode (QNM) spectrum is an important characteristic of a black hole. It dominates the late time response of a black hole to an external perturbation, and, at the same time, does not depend on the way of their excitation. Thus, being dependent on black hole parameters only, the QNMs provide us with the "fingerprints" of a black hole, feasible to be seen in the detection of gravitational waves (for reviews, see [1]). In addition, the importance of the QN spectrum is not limited to the above observational aspects of gravitational waves phenomena. It proved out that in D -dimensional anti-de Sitter space-time, the QNMs of a black hole coincide with the poles of the temperature Green function of the $(D - 1)$ -dimensional conformal field theory [2], [3], [4] (herewith, the temperature of the black hole corresponds to the temperature in the dual field theory within the linear response approach [5]). This led to a new quantitative test of the AdS/CFT correspondence [6]. Along similar lines, support for evidence of the existene of a dS/CFT correspondence [7] were found in [8], [9]. There is also suggestion that the asymptotic quasinormal modes of black holes are connected with the so-called Barbero-Immirzi parameter in Loop Quantum Gravity, which must be fixed to reproduce the Bekenstein-Hawking entropy formula within this theory [10].

All this stimulated considerable interest to study the QNMs of black holes [11]. In particular the QNMs of the Dirac field for different black holes were considered in the papers [12], [14], [15], [17]. Nevertheless, in these papers the study of the Dirac quasinormal modes were limited by *lower overtones*, even though different black hole backgrounds were considered. The low overtones were found for a Schwarzschild black hole in [14], with the help of the third-order WKB method. Soon, it was extended to the case of Schwarzschild-de Sitter black hole [15] using the sixth-order WKB method [16], and also to the case of the charged Dirac field in the background of a charged black hole [17].

In the present paper, we are trying to cover this gap in the study of the Dirac QNMs and shall investigate the *high overtone* behavior of the Dirac perturbations of a Schwarzschild black hole. We observed that at high overtones the imaginary parts of QN spectrum are equidistant with spacing $Im\omega_{n+1} - Im\omega_n = i/8M$. The low overtones can be reproduced with the help of the WKB method, with excellenmt agreement. In addition, we have found the specific modes whith imaginary part $i/8M$ for any multipole number. These modes are, apparently, algebraically special modes discussed, by Chandrasekhar [18].

It is also shown that when increasing the overtone number n , the real part of ω approaches zero. By using the unmodified Fröbenius method, we were able to extend our calculations up to $n = 2000$ only. Therefore, it is possible that at higher n the QN behavior may be different. Nevertheless, we observed a quite stable picture of the QN behavior that seems not to be changed qualitatively at higher overtones.

The paper is organized as follows: in Sec. 2, we review the formulas concerning the Dirac perturbations of a Schwarzschild black hole background. Sec. 3 is devoted to details of Fröbenius technique used here. In Sec. 4, we discuss mod-

erately high overtone behavior, including the above mentioned special modes. In Sec. 5, we study the asymptotically high overtone behavior. Finally, we do some concluding remarks.

2 Dirac perturbation of a Schwarzschild black hole: basic equations

The Dirac equation in an arbitrary curved background has the form [13]:

$$(\gamma^a e_a^\mu (\partial_\mu + \Gamma_\mu) + m) \Psi = 0, \quad (1)$$

where m is the mass of the Dirac field, and e_a^μ is the tetrad field, defined by the metric $g_{\mu\nu}$:

$$g_{\mu\nu} = \eta_{ab} e_\mu^a e_\nu^b; \quad g^{\mu\nu} = \eta^{ab} e_a^\mu e_b^\nu; \quad e_a^\mu e_\mu^b = \delta_a^b; \quad e_\mu^a e_a^\nu = \delta_\mu^\nu,$$

where η_{ab} is the Minkowski metric, γ^a are the Dirac matrices:

$$\{\gamma^a, \gamma^b\} = 2\eta^{ab},$$

and Γ_μ is the spin connection [13]:

$$\Gamma_\mu = \frac{1}{8} [\gamma^a, \gamma^b] g_{\nu\lambda} e_a^\nu e_b^\lambda;_{;\mu}.$$

We will consider here a massless ($m = 0$) field propagating in the Schwarzschild background, whose metric is:

$$ds^2 = f(r) dt^2 - \frac{dr^2}{f(r)} - r^2(d\theta^2 + \sin^2 \theta d\phi^2) \quad , \quad f(r) = 1 - \frac{2M}{r} \quad , \quad (2)$$

where M is the black hole mass.

In this background (2), Eq.(1) leads to

$$\begin{aligned} & \left(\gamma^0 \left(1 - \frac{2M}{r} \right)^{1/2} \frac{\partial}{\partial t} + \gamma^1 \left(1 - \frac{2M}{r} \right)^{1/2} \left(\frac{\partial}{\partial r} + \frac{1}{r} + \frac{M}{2r(r-2M)} \right) + \right. \\ & \left. + \gamma^2 \left(\frac{1}{r} \right) \left(\frac{\partial}{\partial \theta} + \frac{1}{2} \cot \theta \right) + \gamma^3 \left(\frac{1}{r \sin \theta} \right) \frac{\partial}{\partial \phi} \right) \Psi = 0. \end{aligned} \quad (3)$$

This equation can be simplified by the following change

$$\Psi = \left(1 - \frac{2M}{r} \right)^{1/4} \Phi.$$

Then we have

$$\begin{aligned} & \left(\gamma^0 f(r)^{1/2} \frac{\partial}{\partial t} + \gamma^1 f(r)^{1/2} \left(\frac{\partial}{\partial r} + \frac{1}{r} \right) + \gamma^2 \left(\frac{1}{r} \right) \left(\frac{\partial}{\partial \theta} + \frac{1}{2} \cot \theta \right) + \right. \\ & \left. + \gamma^3 \left(\frac{1}{r \sin \theta} \right) \frac{\partial}{\partial \phi} \right) \Phi = 0. \end{aligned} \quad (4)$$

To separate variables we use the following *ansatz*:

$$\Phi(t, r, \theta, \phi) = \frac{1}{r} \begin{pmatrix} iG^{(\pm)}(r)\phi_{jm}^{(\pm)}(\theta, \phi) \\ F^{(\pm)}(r)\phi_{jm}^{(\mp)}(\theta, \phi) \end{pmatrix} e^{-i\omega t}, \quad (5)$$

where

$$\phi_{jm}^{(\pm)} = \begin{pmatrix} \sqrt{\frac{l+1/2+m}{2l+1}} Y_l^{m-1/2} \\ \pm \sqrt{\frac{l+1/2-m}{2l+1}} Y_l^{m+1/2} \end{pmatrix}, j = l \pm 1/2;$$

Then the radial equations can be written as

$$f(r) \left(\frac{d}{dr} - \frac{\kappa_{(\pm)}}{r} \right) F^{(\pm)} = -\omega G^{(\pm)}; \quad (6)$$

$$f(r) \left(\frac{d}{dr} + \frac{\kappa_{(\pm)}}{r} \right) G^{(\pm)} = \omega F^{(\pm)}; \quad (7)$$

$$\kappa_{(\pm)} = \mp(j + 1/2), \quad j = l \pm 1/2. \quad (8)$$

where $\kappa_{(+)}$ and $\kappa_{(-)}$ are negative and positive integers respectively.

Substituting one of the equations into the other, one can find equations with respect to the eigenvalues ω that have the same spectrum:

$$\left(\frac{d^2}{dr^{*2}} + \omega^2 - W^{(\pm)}(r^*)^2 - \frac{dW^{(\pm)}(r^*)}{dr^*} \right) F^{(\pm)}(r^*) = 0; \quad (9)$$

$$\left(\frac{d^2}{dr^{*2}} + \omega^2 - W^{(\pm)}(r^*)^2 + \frac{dW^{(\pm)}(r^*)}{dr^*} \right) G^{(\pm)}(r^*) = 0; \quad (10)$$

with $W^{(\pm)}(r) = \frac{\kappa_{(\pm)}}{r} \sqrt{f(r)}$, and where we have used the tortoise coordinate, defined by $dr^* = \frac{dr}{f(r)}$ ($r^*(r = 2M) = -\infty$, $r^*(r = \infty) = \infty$).

Thus, we are left with a Schrödinger-like wave equation

$$\left(\frac{d^2}{dr^{*2}} + \omega^2 - V(r^*) \right) \Psi(r^*) = 0, \quad (11)$$

where the effective potential has the form

$$V(r) = f(r)\mu \left(\frac{\mu}{r^2} \pm \frac{d}{dr} \sqrt{\frac{f(r)}{r^2}} \right),$$

which vanishes at the both boundaries: $V(r^* = \pm\infty) = 0$. The parameter μ is a positive integer that corresponds to the multipole number. Note that μ is just $|\kappa_{\pm}|$ and κ_{\pm} and is connected with j and l in the formula (8), so that $\mu = l + 1$ for (+) case and $\mu = l$ for (-) case.

3 The continued fraction approach

Under the choice of the positive sign for the real part of ω ($\omega = \omega_{Re} - i\omega_{Im}$, $\omega_{Re} > 0$), QNMs satisfy the following boundary conditions

$$\Psi(r^*) \sim C_{\pm} \exp(\pm i\omega r^*) \quad , \quad r^* \rightarrow \pm\infty \quad , \quad (12)$$

corresponding to purely in-going waves at the black hole event horizon and purely out-going waves at infinity.

Thus, following Leaver [19], we can choose

$$\Psi(r^*) = \exp(i\omega r^*) u(r^*); \quad (13)$$

where $u(r)$ has regular singularity at the event horizon and finite at $r^* \rightarrow \infty$.

The appropriate Fröbenius series then is

$$u(r) = f(r)^{2s} \sum_{n=0}^{\infty} a_n f(r)^{n/2} \quad , \quad (14)$$

where s satisfies the equation

$$f(r)^s \propto \exp(-i\omega r^*), \quad r^* \rightarrow -\infty \quad . \quad (15)$$

From (15), one can find that

$$s = \frac{-i\omega}{f'(2M)} = -2Mi\omega. \quad (16)$$

Substituting (13) and (14) in (11) we obtain the five-term recurrent relation

$$a_n c_0(n, \omega) + a_{n-1} c_1(n, \omega) + a_{n-2} c_2(n, \omega) + a_{n-3} c_3(n, \omega) + a_{n-4} c_4(n, \omega) = 0, \quad (17)$$

where

$$\begin{aligned} c_0(n, \omega) &= \frac{1}{2}n(n - 8Mi\omega); \\ c_1(n, \omega) &= -\mu; \\ c_2(n, \omega) &= 1 - 2\mu^2 - (n - 1 - 8Mi\omega)^2; \\ c_3(n, \omega) &= 3\mu; \\ c_4(n, \omega) &= \frac{1}{2}(n - 8Mi\omega - 4)(n - 8Mi\omega); \end{aligned}$$

The Eq. (17) reduces to the four-term one

$$a_n c'_0(n, \omega) + a_{n-1} c'_1(n, \omega) + a_{n-2} c'_2(n, \omega) + a_{n-3} c'_3(n, \omega) = 0,$$

by the means of the Gaussian elimination:

$$\begin{aligned} c'_0(n, \omega) &= c_0(n, \omega); \\ c'_k(n, \omega) &= c_k(n, \omega), \quad n < 4; \\ c'_1(n, \omega) &= c_1(n, \omega) - c'_0(n - 1, \omega) c_4(n, \omega) / c'_3(n - 1, \omega), \quad n \geq 4; \\ c'_2(n, \omega) &= c_2(n, \omega) - c'_1(n - 1, \omega) c_4(n, \omega) / c'_3(n - 1, \omega), \quad n \geq 4; \\ c'_3(n, \omega) &= c_3(n, \omega) - c'_2(n - 1, \omega) c_4(n, \omega) / c'_3(n - 1, \omega), \quad n \geq 4; \end{aligned}$$

and finally, by means of another Gaussian elimination, to the three-term one:

$$a_{n+1}\alpha_n(\omega) + a_n\beta_n(\omega) + a_{n-1}\gamma_n(\omega) = 0,$$

$$\begin{aligned}\alpha_n(\omega) &= c_0(n+1, \omega); \\ \beta_n(\omega) &= c_1(n+1, \omega), \quad n < 2; \\ \gamma_1(\omega) &= c_1(2, \omega); \\ \beta_n(\omega) &= c_1(n+1, \omega) - \alpha_{n-1}(\omega)c'_3(n+1, \omega)/\gamma_{n-1}(\omega), \quad n \geq 2; \\ \gamma_n(\omega) &= c_2(n+1, \omega) - \beta_{n-1}(\omega)c'_3(n+1, \omega)/\gamma_{n-1}(\omega), \quad n \geq 2;\end{aligned}$$

When ω is the quasinormal frequency, the ratio of the series coefficients is finite and can be found in two ways:

$$\frac{a_{n+1}}{a_n} = \frac{\gamma_n}{\alpha_n} \frac{\alpha_{n-1}}{\beta_{n-1} - \frac{\alpha_{n-2}\gamma_{n-1}}{\beta_{n-2} - \alpha_{n-3}\gamma_{n-2}/\dots}} - \frac{\beta_n}{\alpha_n} = -\frac{\gamma_{n+1}}{\beta_{n+1} - \frac{\alpha_{n+1}\gamma_{n+2}}{\beta_{n+2} - \alpha_{n+2}\gamma_{n+3}/\dots}}. \quad (18)$$

We are left with an implicit continued fraction equation for ω . Then the QNMs will be the roots of the inverted continued fraction above, that is,

$$\beta_n - \frac{\alpha_{n-1}\gamma_n}{\beta_{n-1} - \frac{\alpha_{n-2}\gamma_{n-1}}{\beta_{n-2} - \alpha_{n-3}\gamma_{n-2}/\dots}} = \frac{\alpha_n\gamma_{n+1}}{\beta_{n+1} - \frac{\alpha_{n+1}\gamma_{n+2}}{\beta_{n+2} - \alpha_{n+2}\gamma_{n+3}/\dots}}, \quad (19)$$

that can be solved numerically as soon as $\alpha_n(\omega)$, $\beta_n(\omega)$, $\gamma_n(\omega)$ are found.

4 The Nollert expansion

The convergence of the continued fraction in the right side of (18) becomes worse as the imaginary part of the frequency increases. To circumvent this problem, Nollert proposed to look for an asymptotic approximation for the continued fraction and use it as a starting approximation for the remaining part of the continued fraction (18), at some large index $N \gg n$ [20]. He considered the relation (note that our designations are different from Nollert's ones, who used $C_0(N+1) \equiv \alpha_N$ etc.):

$$R_N(\omega) = \frac{\gamma_N(\omega)}{\beta_N(\omega) - \alpha_N(\omega)R_{N+1}(\omega)}, \quad (20)$$

assuming an expansion in powers of $N^{-1/2}$:

$$R_N(\omega) = C_0(\omega) + C_1(\omega)N^{-1/2} + C_2(\omega)N^{-1} + C_3(\omega)N^{-3/2} + \dots. \quad (21)$$

Note that among the considered fits, the fit in powers of $N^{-1/2}$ is the best one, and, for example, the fit in powers of N^{-1} lead to growing coefficients under the higher terms of the series. If the analytic formulae for β_N and γ_N were known we would find the coefficients directly from (20). But we know that

$$R_N = -\frac{a_N}{a_{N-1}},$$

and we can start from (17) to find R_N :

$$c_0(N)R_N R_{N-1} R_{N-2} R_{N-3} - c_1(N)R_{N-1} R_{N-2} R_{N-3} + c_2(N)R_{N-2} R_{N-3} - c_3(N)R_{N-3} + c_4(N) = 0; \quad (22)$$

From (22) one can find an equation with respect to C_0 :

$$C_0^4 - 2C_0^2 + 1 = 0,$$

which has two solutions, $C_0 = 1$ and $C_0 = -1$. Both of them are valid but both lead to bad approximations. The numerical study gives a more complicated behavior for R_N . It looks like a phase oscillation and we observe that R_N does not converge at infinity but

$$\lim_{N \rightarrow \infty} |R_N| = 1.$$

We do not know the criterion to find its behavior at infinity. It can be, for example,

$$R_N = \pm ie^{i\pi N}, \quad N \rightarrow \infty.$$

Thus, from the above reason it seems we are not able to use the Nollert expansion. That is why in spite of the slow convergence of the continued fractions in the unmodified Fröbenius method we had to be limited by it. This certainly requires much greater computing time to perform the computations.

5 Low overtones

The low overtones can be obtained either with the help of the Fröbenius method or applying the WKB formula at sixth-order [16]. The WKB approach can be applied if the overtone number n is less than the multipole number μ , while the numerical Fröbenius technique does not have this limitation. The first ten overtones we found for $\mu = 1, 2$ are represented in the following tables:

n	Re ω	-Im ω
0	0.182963	0.096982
1	0.125	0.125
2	0.147822	0.316928
3	0.146458	0.424157
4	0.138885	0.549184
5	0.134650	0.674318
6	0.131726	0.799895
7	0.128822	0.925363
8	0.126064	1.050710
9	0.123570	1.176020

n	Re ω	-Im ω
0	0.380037	0.096405
1	0.330719	0.125000
2	0.339865	0.287698
3	0.326095	0.421677
4	0.313180	0.548007
5	0.305740	0.673165
6	0.300096	0.798686
7	0.294725	0.924309
8	0.289734	1.049817
9	0.285201	1.175236

First ten quasinormal frequencies for $\mu = 1$ (left table) and $\mu = 2$ (right table)
Dirac perturbations found by the Fröbenius method.

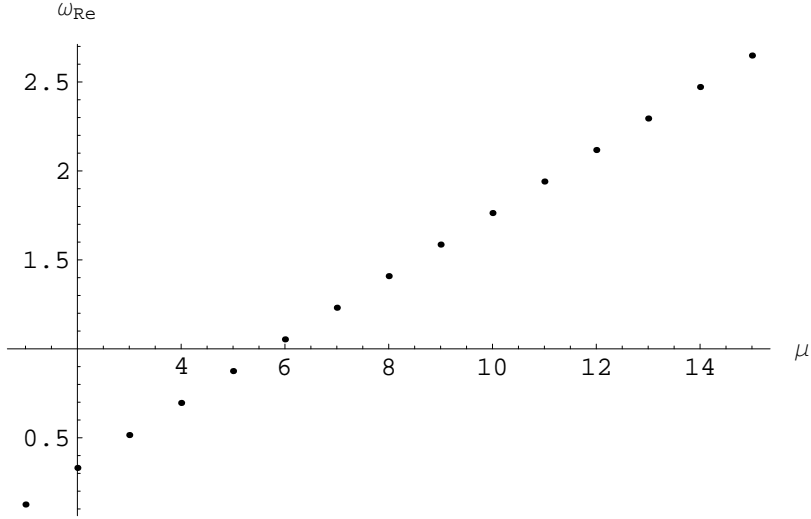


Figure 1: The real part of the QNMs $Re\omega_\mu$ as a function of μ for the "special modes". The imaginary parts $Im\omega_\mu$ of these modes are equal to $1/8M$, no matter the value of μ .

Let us remind that the potentials with opposite chirality produce the same spectrum [14],[15]. That is why we shall consider only positive values of μ . In addition, we observed some "special modes" $\omega = 0.125 - 0.125i$ for $\mu = 1$, $0.330719 - 0.125000$, for $\mu = 2$, etc. These "special modes" have imaginary part $i/8$ (in units where $M = 1$) for *all* multipoles μ . The dependence of the real part of ω for these special modes upon μ is shown on Fig's. 1 and ???. It can be seen that the real part of ω for these "special modes" approach equidistant dependence on μ , as μ is increasing:

$$Re\omega_{\mu+1} - Re\omega_\mu \approx 0.175 \quad , \quad \mu \rightarrow \infty \quad . \quad (23)$$

When n is less than μ we can check our numerical results by the semi-analytic WKB formula up to the sixth-order [16]:

$$i \frac{\omega^2 - V_0}{\sqrt{-2V_0''}} - \Lambda_2 - \Lambda_3 - \Lambda_4 - \Lambda_5 - \Lambda_6 = n + \frac{1}{2} \quad , \quad (24)$$

where V_0 is the height and V_0'' is the second derivative with respect to the tortoise coordinate of the potential at the maximum. The corrections Λ_2 and Λ_3 can be found in [21], whereas Λ_4 , Λ_5 and Λ_6 are presented in [16]; these corrections depend on the value of the potential and higher derivatives of it at its maximum. Note that the WKB approach have been used recently when studying QNMs of different black hole (see for instance [22] and references therein).

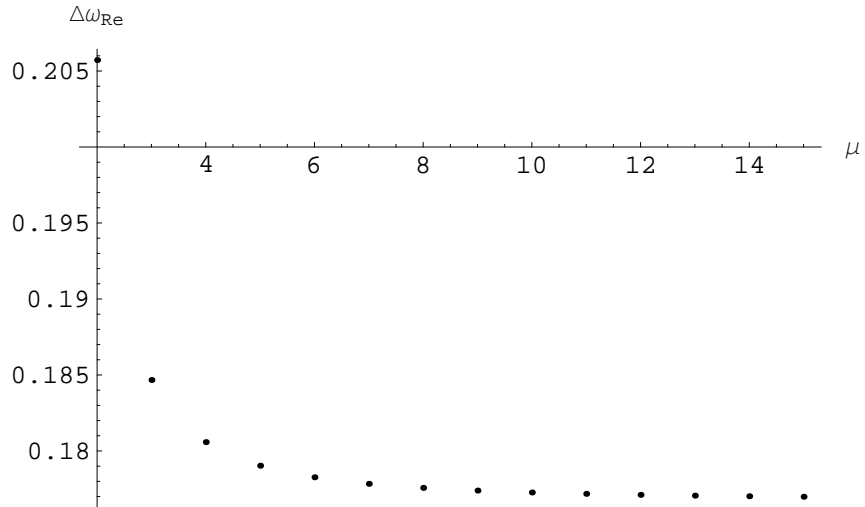


Figure 2: The spacing $Rew_{\mu+1} - Rew_{\mu}$ as a function of μ for the "special modes".

The comparison with numerical results are shown, for instance for the $\mu = 5$ case, in the following table:

n	6th order WKB	Frbenius
0	0.960293-0.096254 i	0.960293-0.096254 i
1	-	0.875000- 0.125 i
2	0.949759-0.290148 i	0.949759-0.290148 i
3	0.929490-0.488114 i	0.929494-0.488116 i
4	0.901072-0.692514 i	0.901129-0.692520 i
5	0.866729-0.905116 i	0.867043-0.905047 i

We see that the special mode $0.875000 - 0.125i$ cannot be reproduced by the WKB technique. From the above table it can be seen that the WKB formula at sixth order confirms the numerical results very well, except for those "special modes" which are apparently algebraically special modes, discussed by Chandrasekhar [18], and are apparently *not* QNMs. It is challenging that the $\mu = 1$ "special mode" equals exactly to $(1/8)(1 - i)$. Analytical solution in this case can possibly be found.

6 High overtones

The main difference from what we know on the high damping regime for perturbations of fields of integer spin (scalar, gravitational, and electromagnetic) is

that now the spacing in imaginary part is not $i/4M$, as it takes place for scalar, electromagnetic, and gravitational perturbations, but $i/8M$. The real part of ω (See Fig. 3 and Fig. 4) falls down quickly to tiny values which already cannot be found with reasonable accuracy by the Fröbenius method. This occurs already at about 400-500 overtones. We have checked that there are no modes with seeming real part at higher overtones, by computing higher than $n = 500$ mode, “jumping” with the step 100 overtones up until $n = 2000$.

Thus, as can be seen from Fig. 3 and 4, $\mu = 1, 2$ QNMs demonstrate the following asymptotic behavior:

$$Re \omega \approx 0 \quad as \quad n \rightarrow \infty \quad , \quad (25)$$

$$Im \omega_{n+1} - Im \omega_n \approx -\frac{i}{8M} \quad as \quad n \rightarrow \infty \quad . \quad (26)$$

The asymptotic QN behavior for higher μ is the same as to that for $\mu = 1, 2$, yet to compute sufficiently high QNMs one by one for higher μ , is a time consuming procedure.

Summarizing all the above results we can conclude that at high overtones

$$Re \omega \approx 0 \quad as \quad n \rightarrow \infty \quad , \quad (27)$$

no matter which the multipole number of the field is. Note that since we could not use the Nollert procedure here, the computing of the sufficiently high overtones took considerable computer time. That is the reason why we could not extend our computation to higher n .

An important question is : which is the criteria that the above picture represents the true asymptotic regime $n \rightarrow \infty$? Certainly, there is no mathematical definiteness here, since the falling of the real part to tiny values does not guaranty that at greater overtone number the real part will not grow. However such a sharp change in asymptotic behavior would look very exotic, after the stable monotonic decreasing we observed. After all, if there were modes with considerable real part at greater overtones, then it would possible to catch them with Fröbenius method, since the more the $Im\omega/Re\omega$ ratio, the greater the length of the continued fraction we must compute.

7 Discussion

In this paper we tried to study the high overtones of the Dirac quasinormal spectrum for a Schwarzschild black hole. The behavior we observed is rather different from that for fields of integer spin. First, the spacing in imaginary part is two times less than that for integer spin fields. Second, while real part of ω for integer spin fields asymptotically approach a constant equal to $\log 3/8M\pi$, the real part for Dirac perturbations goes to zero. Another amazing peculiarity is that the “special modes” have imaginary part equal to $i/8M$, *no matter* the value of the multipole number μ . All this apparently should have some analytical explanation. It is evident that the Dirac QNMs require further investigation

with alternative numerical as well as analytical methods in order to clarify all the above peculiarities of the quasinormal behavior. We hope further investigations will add in obtaining a more complete understanding of the quasinormal behavior in question.

8 Acknowledgements

The work of K. C-B. and R. K. was supported by FAPESP (Brazil). A. Z. thanks xor37h & xbadc0de for their work.

References

- [1] K.Kokkotas and B.Schmidt, "Quasi-normal modes of stars and black holes", *Living.Reviews.Relativ.* **2**, 2 (1999). H-P. Nollert, *Class.Quant.Grav.* **16**, 159 (1999)
- [2] D. Birmingham, I. Sachs, and S.N. Solodukhin, *Phys. Rev. Lett.* **88**, 151301 (2002)
- [3] G.T.Horowitz and V.Hubeny, *Phys. Rev.* **D62** 024027 (2000)
- [4] A.Starinets, *Phys.Rev.D*66:124013, 2002 [hep-th/0207133]
- [5] I.Sachs, hep-th/0312287.
- [6] O. Aharony, S. Gubser, J. Maldacena, H. Ooguri and Y. Oz, *Phys.Rept.*323:183-386,2000 [hep-th/9905111]
- [7] A. Strominger, *JHEP* 0110:034,2001 [hep-th/0106113]
- [8] E. Abdalla, B. Wang, A. Lima-Santos, W.G. Qiu, *Phys.Lett.B*538:435-441,2002 [hep-th/0204030]
- [9] E. Abdalla, K.H.C. Castello-Branco, A. Lima-Santos, *Phys.Rev.D*66:104018,2002 [hep-th/0208065]
- [10] S.Hod *Phys.Rev.Lett.* **81** 4293 (1998); O. Dreyer, gr-qc/0211076.
- [11] E. Berti, K.D. Kokkotas, *Phys.Rev.D*67:064020,2003 [gr-qc/0301052]; S. Das, S. Shankaranarayanan. hep-th/0410209; C.Molina, D.Guingo, E.Abdalla, *Phys. Rev.* **D69** 104013 (2004); R.A.Konoplya and A.Zhidenko, *JHEP* (06) 037 (2004) [hep-th/0402080]; H-B.Zhang, Z-J.Cao, X-F.Gong, W.Zhou, *Class. Quant. Grav.* **21** 917 (2004); V. Cardoso, R. Konoplya and J. P. S. Lemos, *Phys. Rev.* **D** **68** 044024 (2003) [gr-qc/0305037]; R.A.Konoplya, *Phys.Rev.* **D** **66** 084007 (2002) [gr-qc/0207028]; *Phys.Rev.D*70:047503,2004 [hep-th/0406100]; S. Fernando, hep-th/0407062; R.A. Konoplya, *Phys.Rev.D*66:044009,2002 [hep-th/0205142];

Gen.Rel.Grav.34:329-335,2002 [gr-qc/0109096]; hep-th/0410057; G. Siopsis, hep-th/0409262; M.R. Setare, Phys.Rev.D69:044016,2004 [hep-th/0312061]; Mohammad R. Setare, Elias C. Vagenas hep-th/0401187.

- [12] V.Cardoso and J.P.S.Lemos, *Phys .Rev . D* **63** 124015 (2001);
- [13] N.D. Birrell and P.C.W. Davies, *Quantum Fields in Curved Space*, Cambridge Univ. Press, Cambridge (1982)
- [14] H. T. Cho, *Phys .Rev . D* in press gr-qc/0303078
- [15] A.Zhidenko, *Class .Quant .Grav .* **21** 273 (2004)
- [16] R.A.Konoplya, *Phys .Rev . D* **68** 024018 (2003)
- [17] Wei Zhou, Jian-Yang Zhu, *Int.J.Mod.Phys.D*13:1105-1118,2004 [gr-qc/0309071]
- [18] S. Chandrasekhar, *Proc. R. Soc. London A*392, 1 (1984).
- [19] E.M. Leaver, *Proc.Roy.Soc.Lond.A*402:285-298,1985
- [20] Nollert H-P 1993 *Phys. Rev. D* 47 5253
- [21] S. Iyer and C. M. Will, *Phys .Rev . D* **35** 3621 (1987)
- [22] R.A. Konoplya, *Phys.Rev.D*68:124017,2003, [hep-th/0309030]; *Phys.Lett.B*550:117-120,2002 [gr-qc/0210105].

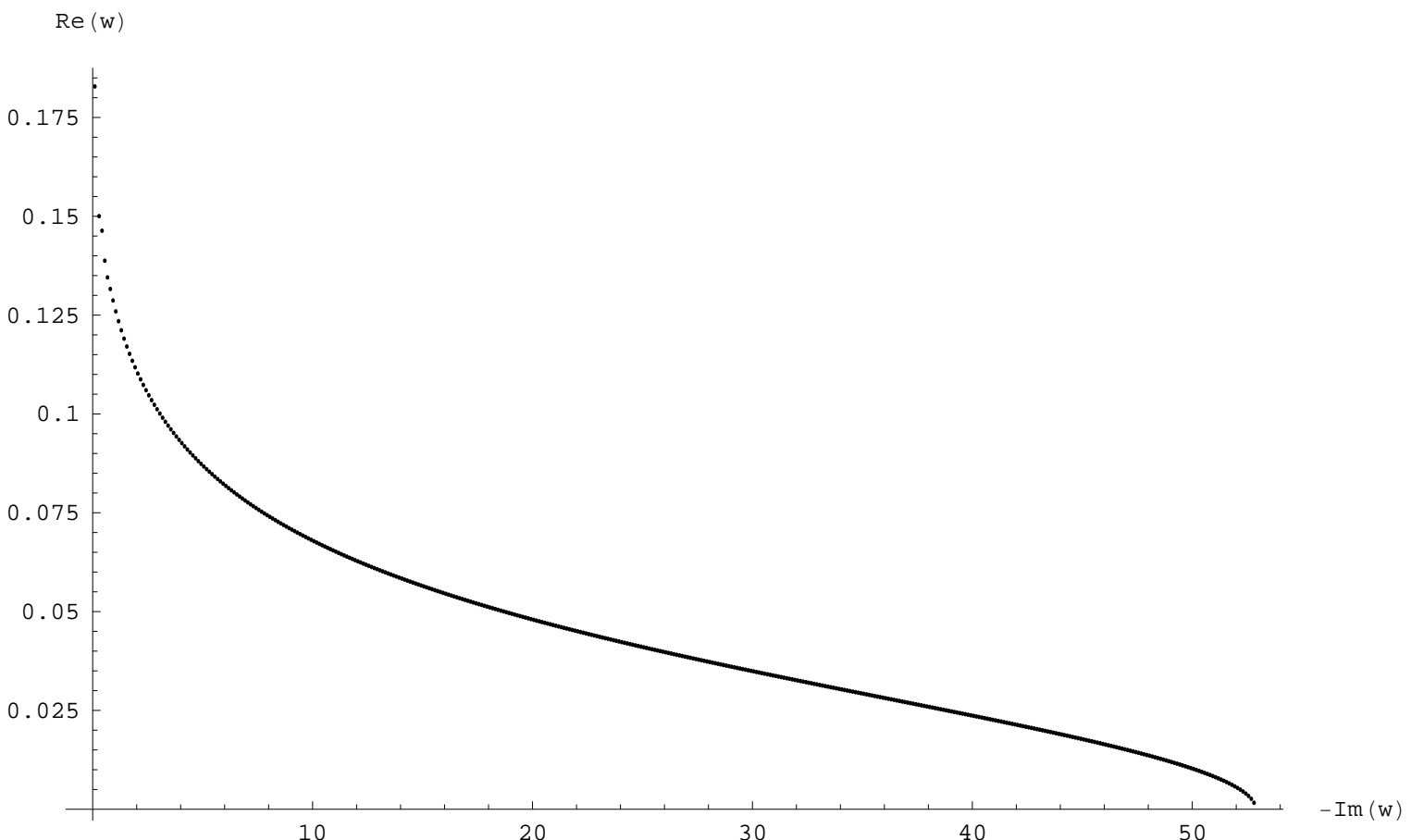


Figure 3: Real part of ω as a function of imaginary part for $\mu = 1$ multi-pole.

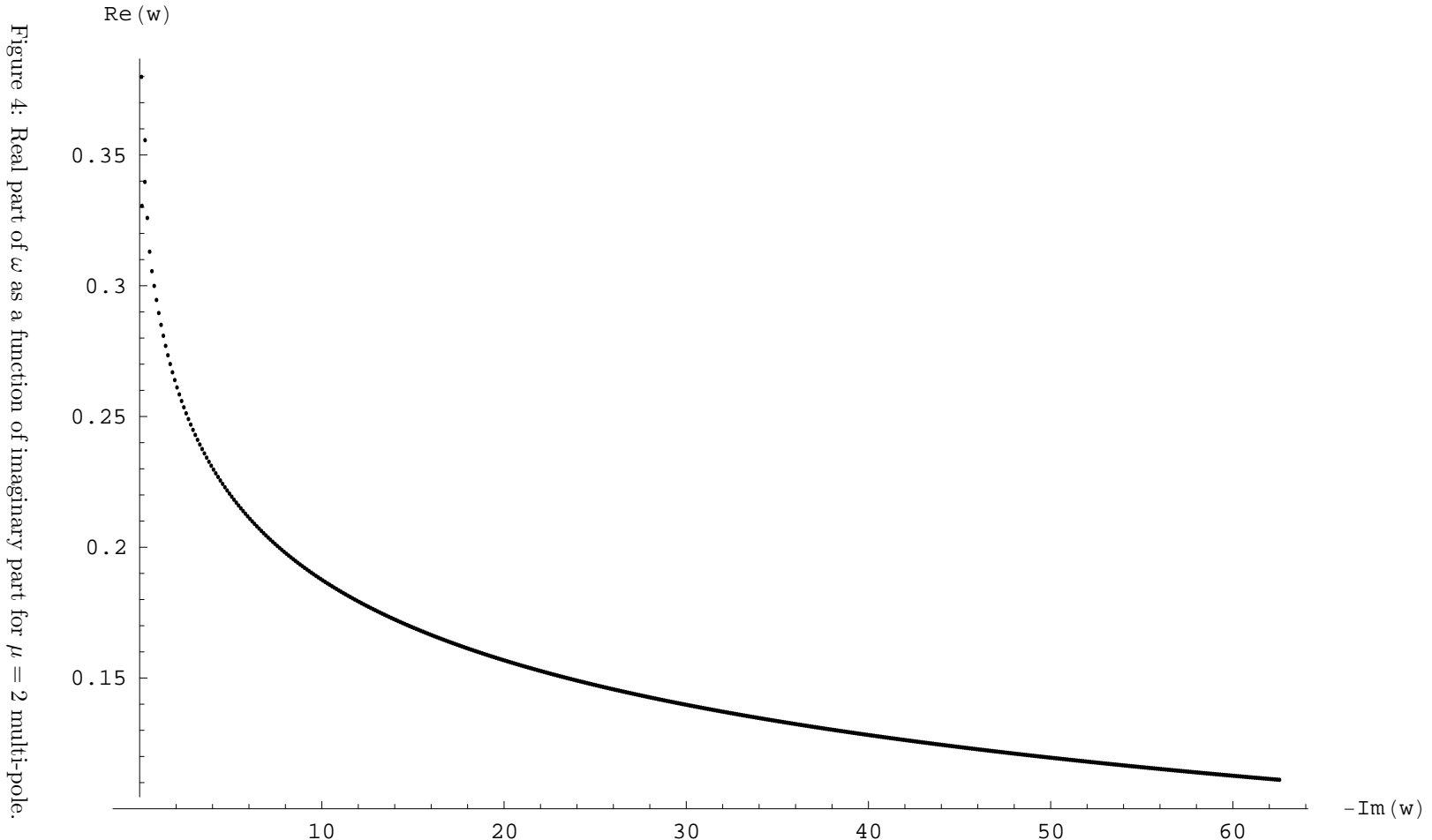


Figure 4: Real part of ω as a function of imaginary part for $\mu = 2$ multi-pole.